CELL-BASED DRUG DEVELOPMENT, SCREENING, AND TOXICOLOGY

STEM CELLS
TRANSLATIONAL MEDICINE

Lithium modulates miR-1906 levels of mesenchymal stem cell-derived extracellular vesicles contributing to poststroke neuroprotection by toll-like receptor 4 regulation

Matteo Haupt[1] | Xuan Zheng[1] | Yaoyun Kuang[1] | Simone Lieschke[1] |
Lisa Janssen[1] | Bert Bosche[2,3,4] | Fengyan Jin[5] | Katharina Hein[1] |
Ertugrul Kilic[6] | Vivek Venkataramani[7] | Dirk M. Hermann[3] | Mathias Bähr[1] |
Thorsten R. Doeppner[1,3,6]

[1]Department of Neurology, University Medical Center Goettingen, Goettingen, Germany

[2]MediClin Clinic Reichshof, Department of Neurocritical Care, First Stage Rehabilitation and Weaning, Germany

[3]Department of Neurology, University Hospital Essen, University of Duisburg-Essen, Essen, Germany

[4]Medical Faculty, Institute of Neurophysiology, University of Cologne, Cologne, Germany

[5]Cancer Center, The First Hospital of Jilin University, Changchun, People's Republic of China

[6]Regenerative and Restorative Medical Research Center, Istanbul Medipol University, Istanbul, Turkey

[7]Institute of Pathology, University Medical Center Goettingen, Goettingen, Germany

Correspondence
Thorsten R. Doeppner, MD, Department of Neurology, University Medical Center Goettingen, Robert-Koch-Str. 40, 37075 Goettingen, Germany.
Email: thorsten.doeppner@med.uni-goettingen.de

Abstract

Lithium is neuroprotective in preclinical stroke models. In addition to that, post-stroke neuroregeneration is stimulated upon transplantation of mesenchymal stem cells (MSCs). Preconditioning of MSCs with lithium further enhances the neuroregenerative potential of MSCs, which act by secreting extracellular vesicles (EVs). The present work analyzed whether MSC preconditioning with lithium modifies EV secretion patterns, enhancing the therapeutic potential of such derived EVs (Li-EVs) in comparison with EVs enriched from native MSCs. Indeed, Li-EVs significantly enhanced the resistance of cultured astrocytes, microglia, and neurons against hypoxic injury when compared with controls and to native EV-treated cells. Using a stroke mouse model, intravenous delivery of Li-EVs increased neurological recovery and neuroregeneration for as long as 3 months in comparison with controls and EV-treated mice, albeit the latter also showed significantly better behavioral test performance compared with controls. Preconditioning of MSCs with lithium also changed the secretion patterns for such EVs, modifying the contents of various miRNAs within these vesicles. As such, Li-EVs displayed significantly increased levels of miR-1906, which has been shown to be a new regulator of toll-like receptor 4 (TLR4) signaling. Li-EVs reduced posthypoxic and postischemic TLR4 abundance, resulting in an inhibition of the nuclear factor kappa-light-chain-enhancer of activated B cells (NF-κB)

signaling pathway, decreased proteasomal activity, and declined both inducible NO synthase and cyclooxygenase-2 expression, all of which culminated in reduced levels of poststroke cerebral inflammation. Conclusively, the present study demonstrates, for the first time, an enhanced therapeutic potential of Li-EVs compared with native EVs, interfering with a novel signaling pathway that yields both acute neuroprotection and enhanced neurological recovery.

KEYWORDS

cerebral ischemia, extracellular vesicles, lithium, mesenchymal stem cells, miR-1906, TLR4

1 | INTRODUCTION

The mood stabilizer lithium has been used for decades for the treatment of bipolar disorders.[1] Lithium, however, has also been recognized to be neuroprotective under experimental disease conditions such as cerebral ischemia, traumatic brain injury, and neurodegeneration.[2-6] Likewise, these experimental findings gave rise to clinical trials, albeit with heterogeneous outcome. Although lithium yielded no beneficial effects in patients suffering from amyotrophic lateral sclerosis,[7] a double-blind, placebo-controlled, randomized clinical trial showed a better neurological outcome in favor of a small subpopulation of stroke patients treated with lithium.[8] However, the overall study population only involved 32 patients treated with lithium and 34 patients treated with placebo, with lithium yielding no beneficial effect in the total study population.

Despite the aforementioned clinical trial from 2014, the data on poststroke brain protection due to lithium are scarce and need further validation. In this context, the majority of experimental stroke studies were performed using prophylactic administration of lithium only, thus not reflecting the clinical situation.[9,10] To the best of our knowledge, only three experimental studies have analyzed the effects of poststroke lithium delivery.[11-13] Identifying a novel GSK3β-independent mechanism, previous work from our group has shown that lithium promotes postischemic neuroprotection and neuroregeneration when applied within a therapeutic time frame of 6 hours.[13]

With lithium enhancing poststroke endogenous neurogenesis,[13] such a mechanism may be of great therapeutic potential. As a matter of fact, the neurogenerative capacity of the adult ischemic brain is utterly diminished, since endogenous neural progenitor cells (NPCs) display both reduced survival rates and low differentiation rates.[14] The application of lithium reverses such effects at least in part. Endogenous neurogenesis, however, is also stimulated upon poststroke transplantation of adult stem cells like mesenchymal stem cells (MSCs) or NPCs,[15-20] which offers an even greater therapeutic time window than the aforementioned 6 hours of lithium. Yet, stem cell transplantation faces the same limitations such as endogenous neurogenesis, including low

Significance statement

The present work, for the first time, indicates an enhanced therapeutic potential of extracellular vesicles (EVs) derived from mesenchymal stem cells preconditioned with lithium against cerebral ischemia. Elucidating a new way of action of such enriched EVs, the present work demonstrates increased intravesicular concentrations of selected miRNAs such as miR-1906. The latter regulates the toll-like receptor 4 and familiar proinflammatory signaling cascades, contributing to enhanced neurological recovery poststroke. Hence, this work provides further and novel evidence for the therapeutic potential of EVs against stroke, paving the way for additional translational studies and clinical trials under stroke settings.

survival rates and reduced differentiation rates of grafted cells. Interestingly, previous work by Linares and Tsai were able to show that in vitro preconditioning of MSCs with lithium results in enhanced efficacy of transplanted MSCs in experimental models of Huntington's disease and stroke, respectively.[21,22]

Although stem cell transplantation has yielded significantly increased neurological recovery in various experimental stroke models with already some clinical trials under way, the underlying mechanisms are obviously indirect. Indeed, recent data have shown that infusion of stem cell-derived conditioned media is not inferior to stem cell transplantation itself.[23-26] Recently, these effects have been attributed to the secretion of extracellular vesicles (EVs) derived from transplanted stem cells. EVs are derivates of late endosomes with a diameter of about 100 to 1000 nm containing a heterogeneous agglomeration of proteins and noncoding RNAs.[27] The application of EVs results in better neurological outcome in experimental stroke models,[23,28-30] albeit fundamental questions still have to be addressed. Hence, the present work analyzes both mechanisms and effects of MSC-derived EVs obtained from MSC in vitro

preconditioning with lithium in a mouse model of focal cerebral ischemia.

2 | MATERIALS AND METHODS

2.1 | C57BL6 bone marrow-derived MSCs

Cryopreserved bone marrow-derived MSCs (mentioned as "MSCs" only) were obtained from Cyagen (https://www.cyagen.com/us/en/product/c57bl6-mesenchymal-stem-cells.html). According to the manufacturer, the cells have been characterized for expression patterns of defined surface markers found on MSCs. Flow cytometry analysis performed by the manufacturer revealed MSCs to be positive for CD34, CD44, and Sca-1 as well as being negative for CD117. The cells were plastic adherent and showed multipotential differentiation abilities along osteogenic, chondrogenic, and adipogenic lineages. These bone marrow-derived MSCs were grown in standard growth media consisting of DMEM/F-12 GlutaMAX supplemented with 10% fetal bovine serum (FBS) and 5 µg/mL gentamicin (Invitrogen Life Technologies, Carlsbad, California). The cell cultures were incubated under standard cell culture conditions, that is, cells were kept at $37^\circ C$ in a humidified atmosphere containing 5% CO_2. For experiments, only cells from passages 3 to 5 were used. Differences in morphology, proliferation, and MSC surface marker expression were not observed in these cells.

2.2 | In vitro preconditioning of MSCs with lithium

MSCs were treated with lithium chloride (Sigma-Aldrich, St. Louis, Missouri) or saline as control, using a slightly modified protocol published before.[22,31] Briefly, the preconditioning paradigm included incubation of MSCs from passages 3 to 5 with lithium chloride for 24 hours at a final concentration of 2.5 mM. Thereafter, lithium was washed out, and the cells received fresh cell culture medium without lithium chloride. Following the preconditioning paradigm, supernatants of so treated MSCs were harvested after an additional incubation for 2 days in order to enrich for EVs as described in Section 2.3.

2.3 | EV preparation from conditioned medium using polyethylene glycol

Enrichment of EVs essentially followed our protocol as previously described.[32] Conditioned medium derived from the aforementioned MSCs was centrifuged at $10000g$ in a 5810R centrifuge (Eppendorf, Hamburg, Germany). The supernatants were then supplemented with stock solutions of polyethylene glycol (PEG) 6000 (Sigma, Neustadt, Germany) to final concentrations of 12% PEG. Samples were mixed gently by inverting the tubes three times and then stored at $4^\circ C$ for up to 12 hours, that is, overnight. EVs were concentrated by centrifugation at $1500g$ for 30 minutes at $4^\circ C$. Supernatants were removed and pellets resuspended in 1 mL of phosphate-buffered saline (PBS). To remove residues of PEG from the suspension, the EV-enriched fractions were washed with 9 mL PBS (total volume of 10 mL) and ultracentrifuged at $110\,000g$ for 2 hours at $4^\circ C$. The resulting pellet was resuspended in 250 µL of PBS. Obtained EV samples were stored at $-80^\circ C$.

2.4 | Characterization of MSC-derived EVs

Nanosight tracking analysis (NTA) and Western blots were performed to ensure sufficient quality of enriched MSC-derived EVs. NTA (Particle Metrix, Meerbusch, Germany) was done for both size determination and quantification analysis of enriched EVs, as shown previously.[33] As such, 1:1000 water-diluted samples were measured in duplicate, and 400 µL of the diluted sample was injected into the measurement chamber. Each sample was measured three times, and the length of the video of each measurement was set to 30 seconds.

Using as additional internal quality control and also with regard to the impact of lithium incubation on EV secretion patterns, NTAs were also performed immediately before incubation of MSCs with lithium or PBS (basal level), at 12 and 24 hours after the beginning of lithium/PBS treatment. Finally, we also measured EV concentrations in samples 24 hours after treatment of MSCs with either lithium or PBS (ie, 48 hours after the beginning of the treatment). The basal value (before treatment) showed peak values of 4.4×10^6 at 130 nm in size, whereas peak values at 12 hours after the beginning of the treatment were 5.1×10^6 at 120 nm (lithium group) and 5.4×10^6 at 140 nm (PBS group), respectively. At 24 hours after the beginning of the treatment peak values were 6.0×10^6 at 130 nm (lithium group) and 5.8×10^6 at 120 nm (PBS group), showing no significant difference between the two treatment groups. At 48 hours after the beginning of the treatment (ie, 24 hours after the end of the treatment), peak values differed significantly between each other with 7.4×10^6 at 130 nm (lithium group) and 5.6×10^6 at 130 nm (PBS group), respectively. Further experiments were, however, always performed with EVs obtained 48 hours after the end of the lithium or PBS treatment (72 hours after the beginning of the treatment) where the significant differences between the two groups were even greater (see Figure S2).

For Western blots, protein concentrations of EV samples were measured using the microbicinchoninic acid assay (Thermo Fisher Scientific, Waltham, Massachusetts), and blots were performed using 5 µg of concentrated EV fractions. The latter were treated with sample buffer (dithiothreitol, 0.1% sodium dodecyl sulfate (SDS), 0.1 M Tris HCl; pH 7.0) and boiled for 5 minutes at $95^\circ C$ before separation on a 12% SDS-polyacrylamide gel electrophoresis. The samples were transferred to polyvinylidene fluoride membranes (Merck Group, Darmstadt, Germany), and the membranes were stained with antibodies recognizing "exosomal marker" proteins such as CD63 (1:500, Biorbyt, Cambridge, UK), TSG101 (1:500, GeneTex, Irvine, California), and Hsp70 (1:1000, Abcam, Cambridge, UK) overnight. Thereafter, membranes were incubated for 1 hour with a matched horseradish peroxidase-labeled secondary antibody. Immunoreactivity was detected using chemiluminescence detection kit reagents and a ChemiDoc Station (Bio-Rad, Hercules, California). Western blotting procedures were repeated four times per sample.

2.5 | Oxygen-glucose deprivation and cell culture of neurons, astrocytes, and microglia

Cortical neurons were obtained from male C57BL6 E17 embryos. Astrocytes and microglia were isolated from new born mice 24 hours after birth. Briefly, tissue from the cortex was digested by means of trypsin 0.125% (Invitrogen Life Technologies). The tissue was homogenized and filtered with a 100-μm cell strainer (Biologix, Köln, Germany). Thereafter, cells were centrifuged and resuspended in Dulbecco's modified Eagle's medium (Invitrogen Life Technologies) containing both 10% FBS (Invitrogen Life Technologies) and penicillin-streptomycin (Invitrogen Life Technologies). An amount of 10^6 neurons per milliliter was seeded on six-well plates for which a total volume of 2 mL per well was used. Two hours after seeding, the cell culture medium was exchanged to neurobasal medium (Invitrogen Life Technologies), which included 1% L-glutamate and 2% B27. Astrocytes and microglia were seeded in flasks (Sigma-Aldrich) coated with poly-L-lysine (Sigma-Aldrich) in order to obtain mixed glial cultures. After 3 days, the cells reached confluency. The flasks were then shaken overnight at 200 rpm and adherent cells (astrocytes) were reseeded in cell cultures dishes, whereas floating cells (microglia) were collected and seeded in six-well plates to obtain microglia.

Oxygen-glucose deprivation (OGD) was essentially performed as described before by our group.[13] Briefly, the cells were incubated in Sterofundin medium (Braun, Melsungen, Germany) containing 1 mM mannitol and incubated at 37°C in a hypoxic chamber with 1% O_2 and 5% CO_2 (remainder N_2) for 60 minutes (neurons), 8 hours (microglia), or 12 hours (astrocytes). Thereafter, the cells were reincubated under standard cell culture conditions for 24 hours. As for neurons, the treatment with EVs (2×10^6 cell equivalents for each condition or 13.5 μg EV protein) started either at the beginning of hypoxia or at the beginning of reoxygenation. EV treatment of astrocytes and microglia was always done at the beginning of reoxygenation. Controls received PBS at the corresponding time points. Cell viability was assessed using a Live/Dead Viability/Cytotoxicity kit (Cambrex, Wiesbaden, Germany).

2.6 | Induction of MCAO and injection of EVs

Experimental procedures following the ARRIVE and STAIR recommendations were carried out according to the guidelines for the care and health of animals and were approved by local authorities. All mice received a periprocedural analgesic treatment by means of buprenorphine (0.1 mg/kg body weight (BW)) and carprofen (5 mg/kg BW). The latter was also given on the two consecutive days after surgery. Using a power calculation with the value of 0.8 and an effect size between 0.25 and 0.4, mice were randomly allocated to the experimental treatment groups. As such, Irina Graf (IG, see Acknowledgment) ordered animals and formed the experimental groups in question according to the power calculation before the beginning of any experiments. IG was not involved in any further part of the study. All analysts were blinded from the study, since the surgeons were not

involved in the processing of the data. Precise numbers of animals used for data analysis are given in the appropriate figure legends. Also refer to Figure S1 for an overview of the experimental paradigm.

Middle cerebral artery occlusion (MCAO) was induced in male C57BL6 mice weighing 26-29 g with a duration of cerebral ischemia of 60 minutes as previously described.[34] The surgery was performed under constant anesthesia with isoflurane (1-1.5%) as well as under laser Doppler control. For transient occlusion of the MCA, a silicon-coated nylon monofilament (Doccol, Sharon, Massachusetts) was used. Sham animals underwent the very same procedure, but without insertion of the nylon filament.

EVs were systemically delivered to mice via intravenous injection on days 1, 3, and 5. All mice received the same concentration of EVs, that is, 2×10^6 cell equivalents corresponding to 13.5 μg of total protein. A volume of 100 μL was injected under anesthesia on day 1 poststroke via catheterization of the right femoral vein, whereas injections on day 3 and on day 5 (also 100 μL of volume) were done choosing the retroorbital delivery route. Controls received PBS at the time points given, using the same delivery routes as described for EVs. For short-term experiments with a survival period of 2 days only, mice only received one intravenous injection of either PBS, EVs, or Li-EVs via cannulation of the right femoral vein on day 1 poststroke.

2.7 | Analysis of poststroke brain injury and neuroregeneration

Neuroregeneration was assessed by analyzing co-expression of bromodeoxyuridine, which was given to mice by intraperitoneal injection (50 mg/kg BW) on days 8 to 28, with markers of both angiogenesis and neurogenesis. Three months after induction of stroke, mice received transcardial perfusion with 4% paraformaldehyde in 0.1 M PBS and immunohistochemical analysis was performed on coronal cryostat sections using the following primary antibodies: monoclonal mouse anti-BrdU (1:400; Roche, Mannheim, Germany), monoclonal rat anti-BrdU (1:400; Abcam), polyclonal goat antidoublecortin (Dcx; 1:50; Santa Cruz Biotechnology, Heidelberg, Germany), monoclonal mouse anti-NeuN (1:1000; Merck Millipore, Darmstadt, Germany), polyclonal chicken anti-glial fibrillary acidic protein (GFAP; 1:1000; Merck Millipore), polyclonal rabbit anti-CNPase (1:250, Sigma-Aldrich), and monoclonal rat anti-CD31 (1:200; BD Biosciences, Heidelberg, Germany). Following detection with appropriate secondary antibodies, quantitative analysis was performed using regions of interest within the ischemic lesion site as previously described.[16] In detail, cell count analysis within the basal ganglia was done at 0.14 mm anterior, 2.5 to 3.25 mm ventral and 1.5 to 2.25 mm lateral from bregma (see Figure S1 for a sketch as well). Neuronal densities were determined to indicate the extent of chronic brain injury and were also multiplied with striatal areas of each section, thus correcting for consequences of brain atrophy as described by group elsewhere.[35] GFAP staining analysis was used in order to assess glial scar formation, whereas axonal density was analyzed in order to indicate axonal plasticity as explained afore.[16]

2.8 | Assessment of poststroke neurological recovery

Behavioral tests were performed for assessing long-term neurological outcome in stroke mice during an observation period of 3 months. The mice received training 1 to 2 days before induction of MCAO in order to ensure proper test performance. These tests included the rota rod test, the tight rope test, the corner turn test, and the balance beam test and were performed as previously described.[36] Although a recent discussion with regard to the suitability of certain behavioral tests for the assessment of neurological recovery at chronic stroke stages exists,[37] these tests have been proven to be sensitive for our stroke model. Briefly, the readout parameter for the rota rod test, which was performed in duplicate, was the time the animal spent on the rotating rod. The maximum testing time was 300 seconds. The tight rope test (like the balance beam test) was performed twice per time point as well. Mice were scored from 0 (minimum) to 20 (maximum), depending on the time they needed to reach either side of the two platforms and whether or not they fell from the rope during the test time of 60 seconds. For the balance beam test, the time until the animal reached the platform was measured. The maximal testing time was 60 seconds as well. In the corner turn test, the laterality index was calculated out of 10 trials per time point, with a score of 0.5 indicating no neurological impairment and a score of 1 indicating severe neurological impairment. Single data of the extensive behavioral test analyses are not provided in the manuscript itself because of its huge data amount, which is available on request from the corresponding author.

2.9 | Determination of (sub)acute brain injury

Mice were sacrificed on either day 2 or on day 6 after stroke induction. Infarct volumes were calculated by staining brain tissue with triphenyltetrazolium chloride on 2-mm-thick brain slices. The latter were used for calculation of hemispheric infarct volumes using Image J software. Moreover, (sub)acute brain injury was analyzed using terminal deoxynucleotidyl transferase dUTP nick end labeling (TUNEL) staining on coronal cryostat sections processed as stated in Section 2.7, following the manufacturer's kit instructions (R&D Systems, Wiesbaden, Germany). The subsequent analysis was done in the same coordinates as mentioned above.

2.10 | Measurement of proteasome activity

The proteasome activity was performed as previously described.[38] Very briefly, enzyme activity was measured in left ischemic hemispheres from which homogenates were generated 48 hours poststroke. The homogenates were made using a lysis buffer that contained 100 mM Tris-HCl, 145 mM NaCl, 10 mM ethylenediaminetetraacetic acid (EDTA), and 0.5% Triton X-100 at pH 7.5. The chymotrypsin-like activity of the proteasome was measured using Suc-LLVY-AMC (50 μM; Sigma-Aldrich). The latter was incubated in a volume of 90 μL of reaction buffer (50 mM

Tris, 20 mM KCl, 1 mM magnesium acetate, 2 mM dithiothreitol, 1 mM leupeptin, 1 μg/mL aprotinin [Sigma-Aldrich] and 1 mM phenylmethylsulfonyl fluoride [Merck]). Substrate cleavage was evaluated at 37°C in a fluorescence microtiter plate reader at $\lambda_{exc.}$ = 355 nm and at $\lambda_{em.}$ = 460 nm. During the straight proportional phase of the enzyme kinetics between 8 and 14 minutes, the delta of such a reaction was calculated. Values are given as arbitrary fluorescence units per min per mg protein, which was determined by means of the Bradford assay.

2.11 | Detection of selected growth factor and cytokines

As previously described,[14] brain-derived neurotrophic factor (BDNF; Promega, Walldorf, Germany), glial cell line-derived neurotrophic factor (GDNF; Promega), vascular endothelial growth factor (VEGF; R&D Systems), basic fibroblast growth factor (R&D Systems), and epidermal growth factor (EGF; R&D Systems) was measured by enzyme linked immunosorbent assay (ELISA) in left (ischemic) hemispheres 84 days after MCAO. As for the detection of tumor necrosis factor-α (TNF-α), another ELISA assay from R&D systems was performed on day 2 in ischemic brain hemispheres.

2.12 | Analysis of poststroke inflammatory responses

Flow cytometry analysis from both blood and brain samples was performed on day 2 and on day 6 poststroke using a previously described protocol.[16,23,39] Using blood samples, leukocytes were purified by means of a lysis buffer that consists of 155 mM NH_4Cl, 10 mM $KHCO_3$, and 3 mM EDTA. On the contrary, left ischemic brain hemispheres were mechanically homogenized in a buffer of collagenase type XI (125 U/mL), hyaluronidase (60 U/mL), and collagenase (450 U/mL) in Ca^{2+}/Mg^{2+}-supplemented PBS (Sigma-Aldrich). Thereafter, the samples were incubated with the antibody in question as described afore.[23] Absolute cell numbers were measured using CountBright counting beads (Invitrogen Life Technologies).

2.13 | Analysis of oxidative stress

Thiobarbituric acid reactive substances (TBARS) were measured on day 2 in brain lysates, indicating lipid peroxidation of membranes and thus oxidative stress.[14] TBARS such as malondialdehyde (MDA) react with thiobarbituric acid resulting in a chromogenic compound. Photometric measurement was done at λ = 532 nm. TBARS formation is expressed as MDA equivalents using 1,1,3,3-tetramethoxypropan as standard.

2.14 | Western blotting experiments

A plethora of Western blot analyses was performed from cell lysates after OGD (see above) and from ischemic left hemispheres at 2 days after stroke

induction, using formerly described protocols from our group with slight modifications.[40] Lysates obtained using a buffer containing 50 mmoL/L Tris, pH 8.0, 150 mmoL/L NaCl, 1% Triton X-100, and protease inhibitors were centrifuged and used for polyacrylamide gel electrophoresis. Following transfer to polyvinylidene fluoride membranes, proteins were incubated overnight at 4°C with a monoclonal mouse anti-nuclear factor kappa-light-chain-enhancer of activated B cells (NF-κB) p65 (1:200; Santa Cruz Biotechnology), a monoclonal mouse anti-IκB-α (1:1000; Santa Cruz Biotechnology), a polyclonal rabbit anti-inducible NO synthase (anti-iNOS; 1:500; Santa Cruz Biotechnology), a polyclonal rabbit cyclooxygenase-2 (COX-2; 1:1000; Santa Cruz Biotechnology), and a polyclonal rabbit anti-toll-like receptor 4 (anti-TLR4) (1:1000; Santa Cruz Biotechnology) antibody. Membranes were rinsed, incubated with secondary peroxidase-coupled goat anti-rabbit or goat anti-mouse antibody (1:2000; Santa Cruz Biotechnology), rinsed, immersed in ECL solution and exposed to ECL-Hyperfilm (Amersham Biosciences, Freiburg, Germany). Protein loading was controlled using a monoclonal mouse anti-β-actin antibody (1:5000; Sigma-Aldrich). Membranes were scanned and used for densitometric analysis. In the same tissue samples, NF-κB p65 translocation from the cytosol toward the nucleus, which reflects NF-κB activation, was evaluated using a commercially available kit (FIVEphoton Biochemicals, San Diego, California) following the manufacturer's protocol. Whole uncropped representative blots are also shown in Figure S5.

2.15 | Real-time polymerase chain reaction

For detection of selected miRNAs, generation of cDNA from these aforementioned miRNAs was achieved using a TaqMan miRNA real-time reverse transcriptase (RT) kit obtained by Thermo Fisher Scientific. The assays were performed according to the manufacturer's protocols as essentially explained before.[41,42] The miRNAs measured were not only chosen by mere increased probability of being enriched in MSC-derived EVs as reviewed elsewhere.[43] Rather, these miRNAs were chosen according to previous reports published or due to own unpublished reports in the context of cellular protection against cardiovascular diseases and/or neurodegeneration. Without attempting to be exhaustive, our analysis therefore focused on miR-132,[44-46] miR-1906,[47] miR-126,[48-50] miR-222,[51] miR-21,[52,53] and miR-23.[54]

Individual miRNA detection was done using a forward primer and a 3′ universal reverse primer provided by the RT kit. qPCR using an SYBR Green Master Mix (Applied Biosystems, Foster City, California) was performed employing the Applied Biosystems instrument. The amplification conditions included 1 cycle of 50°C for 2 minutes and 1 cycle of 95°C for 10 minutes, followed by 40 cycles of 95°C for 30 seconds and 55°C for an additional minute. Specificity was verified by melt curve analysis. The relative quantitation of miRNAs was normalized by the ΔΔCt method.

2.16 | Statistics

The results are presented as mean ± SD. All data were normally distributed as indicated by the Kolmogorov-Smirnov test. Accordingly, parametric tests were applied. For comparisons between two groups, statistical comparisons were done using the Student t tests. For comparison between multiple groups, a one-way ANOVA followed by the Tukey's post hoc test was used. P values of <.05 were considered to be statistically significant.

3 | RESULTS

3.1 | Lithium preconditioning of MSCs enhances the therapeutic potential of MSC-derived EVs against OGD injury of cultured neurons

We first analyzed whether or not lithium preconditioning of MSCs affects the therapeutic potential of MSC-derived EVs, using an OGD assay on primary cortical neurons (Figure 1). The latter were exposed to OGD for 1 hour followed by reoxygenation under standard cell culture conditions for 24 hours. Cells that were treated with PBS only (controls) displayed a profound cell death rate. On the contrary, incubation of neurons with native MSC-derived EVs at the beginning of the OGD, that is, EVs derived from MSCs that were not treated with lithium ("EVs"), significantly reduced neuronal cell injury (Figure 1A). The treatment of such hypoxic neurons with EVs derived from MSCs that had been treated with lithium before ("Li-EVs"), however, yielded an even more pronounced neuroprotection. Likewise, EV-treatment starting at the beginning of reoxygenation also resulted in significant neuroprotection, with an even more favorable outcome in the Li-EVs group (Figure 1B).

3.2 | Neurological recovery is further enhanced after treatment with Li-EVs

The aforementioned experiments have shown that lithium alters the secretion patterns of MSCs with regard to EVs, resulting in a more pronounced neuroprotection against OGD in comparison with native EVs in vitro. In light of previous work from our group demonstrating that native EVs enhance neurological recovery after stroke, we next wondered whether or not Li-EVs can enhance these effects even further. Indeed, treatment with EVs yielded better neurological recovery after stroke induction in comparison with control animals that had been treated with saline, as analyzed by four well-established behavioral tests (Figure 2). Treating stroke animals with Li-EVs, however, significantly improved the poststroke functional outcome when compared with both nontreated mice and mice that had received native EVs. Of note, early test scores taken during the EV treatment period itself, that is, on days 2 and 4 poststroke, only partially showed better test performance of mice treated with either EVs or Li-EVs (Figure S4).

Analysis of brain injury 3 months after stroke induction revealed significantly reduced brain injury in mice treated with Li-EVs in comparison with controls and to mice treated with native EVs, albeit the latter also showed significantly reduced brain injury when compared
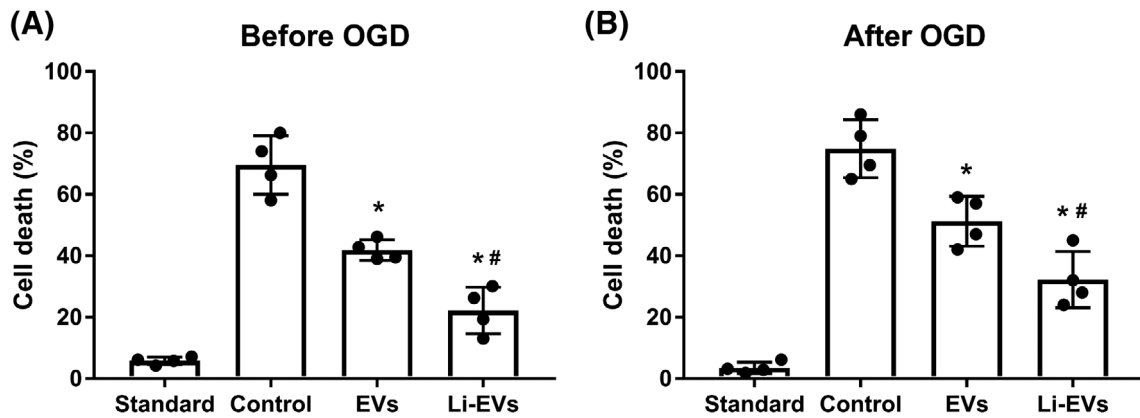
FIGURE 1 Lithium preconditioning of MSCs enhances therapeutic potential of MSC-derived EVs against OGD injury of cultured neurons. Cortical neurons were exposed to OGD for 1 hour followed by reoxygenation under standard cell culture conditions for 24 hours. Treatment with PBS (control), EVs or Li-EVs started either at the beginning of the OGD, A, or after the OGD, B, that is, at the beginning of the reoxygenation. Cells referred to as "standard" were not exposed to OGD but kept under standard cell culture conditions. *Significantly different from controls ($P < .05$). #Significantly different from neurons treated with EVs ($P < .05$). n = 4 per condition. EVs, extracellular vesicles; Li-EVs, lithium-treated EVs; MSCs, mesenchymal stem cells; OGD, oxygen-glucose deprivation; PBS, phosphate-buffered saline

with controls. En detail, neuronal densities were 435.6 ± 31.5 NeuN⁺ cells per mm² (controls), 665 ± 40.8 NeuN⁺ cells per mm² (EVs), and 876 ± 56.2 NeuN⁺ cells per mm² (Li-EVs). In line with this, both glial scar formation (expressed as number of GFAP⁺ cells per mm²) and poststroke brain atrophy (expressed as percentage of ipsilateral striatal volume compared with contralateral volumes) were significantly decreased due to EV treatment and even more so due to Li-EV treatment in comparison with controls 3 months poststroke. As for glial scar formation, we found values of 67.8 ± 8.3 (controls), 51.6 ± 7.8 (EVs), and 34.7 ± 6.1 (Li-EVs). Analysis of ipsilateral brain atrophy revealed values of 52.4 ± 2.7 (controls), 64.2 ± 5.3 (EVs), and 70.5 ± 9.7 (Li-EVs).

3.3 | Li-EVs help boost poststroke neuroregeneration

Enhanced neurological recovery after stroke can be a consequence of either acute neuroprotection or neuroregeneration. The latter has already been shown by our group for native MSC-derived EVs.[23] Herein, we demonstrate that Li-EVs further increase poststroke neurogenesis, angiogenesis, and axonal plasticity, confirming the aforementioned results on poststroke neurological recovery (Figure 2). To be precise, an analysis of BrdU positive cells 3 months after stroke induction revealed a significantly increased co-localization with Dcx, CNPase, NeuN, and CD31 (Figures 3A and S3A-E). Likewise, an enhanced level of axonal plasticity was observed in animals treated with Li-EVs when compared with both controls and mice treated with EVs (Figure 3B). Although new born cells are known to be not integrated in the residing poststroke neural network,[14] these cells are able to indirectly modify their extracellular milieu as indicated by different concentration patterns of cytokines and growth factors. Indeed, treatment with Li-EVs increased the concentration of selected growth

factors within the ischemic milieu 3 months after stroke induction (Figure 3C and S3F-J).

3.4 | Lithium preconditioning affects MSC secretion patterns

In light of the aforementioned therapeutic effects of Li-EVs against both in vitro OGD and cerebral ischemia of mice, we next characterized basic properties of Li-EVs with regard to EV concentration, size, and expression profiles of "exosomal" markers. NTA analysis (Figure S2A) revealed particle sizes of 130 nm (Li-EVs) and 120 nm (EVs) at which EV concentrations reached their maximum. These data are in line with medium-sized EVs among which are exosomes.[27] In this context, Western blot analysis of "typical" EV-associated proteins[27] revealed abundance of Hsp70, TSG101, and CD63, with no difference between the two EV fractions (Figure S2B).

Since miRNA contained within secreted EVs are regarded to be key players mediating biological properties of EVs,[55] we next analyzed selected miRNAs that are known to be enriched in MSC-derived EVs and/or play significant roles in models of cardiovascular diseases or neurodegeneration as stated in Section 2. As such, we detected miR-21, miR-222, miR-23, and miR-126 within both control EVs and Li-EVs, albeit no significant difference was observed between these two EV groups (Figure 4). On the contrary, concentrations of both miR-132 and miR-1906 were significantly increased in Li-EVs (Figure 4). In light of previous work from our group, however, application of an ectopic miR-132 containing viral vector did not yield neuroprotection against focal cerebral ischemia (own unpublished observation) in contrast to viral vectors containing other miRNAs such as miR-124.[56] We therefore focused on the lithium-associated increase of miR-1906 for the remainder of the present study.
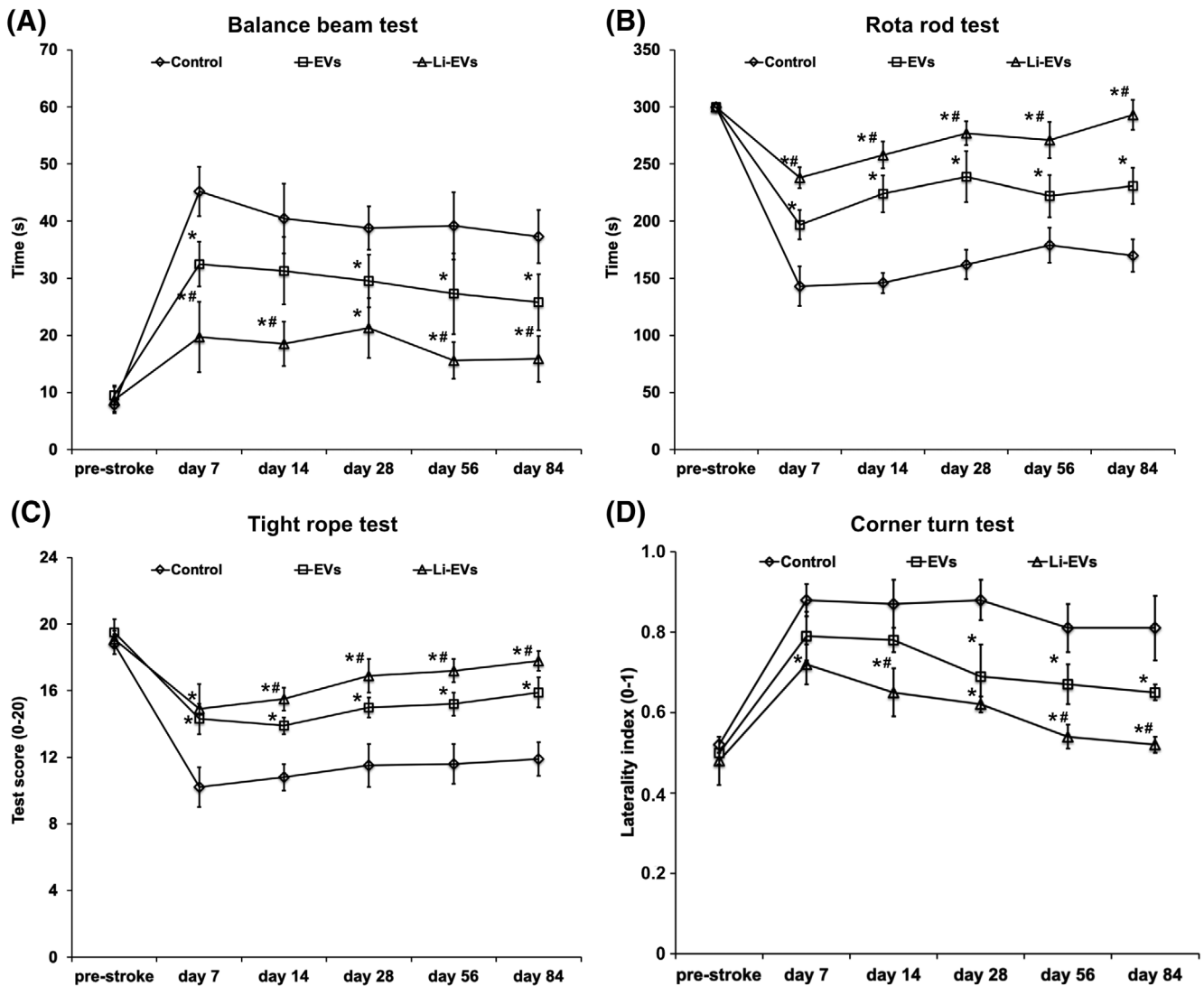
FIGURE 2 Treatment with Li-EVs results in enhanced poststroke neurological recovery. Mice were exposed to middle cerebral artery occlusion followed by intravenous delivery of PBS (control), native EVs (EVs), or Li-EVs on days 1, 3, and 5. During the observation period of 3 months, mice were submitted to the balance beam test, A, the rota rod test, B, the tight rope test, C, and the corner turn test, D. Note that for the rota rod test, the maximum test time was 300 seconds, and only healthy mice that stayed on the rod for this period of time were used for the test. *Significantly different from controls ($P < .05$). #Significantly different from mice treated with native EVs ($P < .05$). n = 18 for controls, n = 21 for EVs, and n = 20 for Li-EVs. EVs, extracellular vesicles; Li-EVs, lithium-treated EVs; PBS, phosphate-buffered saline

3.5 | miR-1906 containing Li-EVs regulate poststroke injury via regulation of TLR4

The miR-1906 has recently been identified as a novel regulator of the TLR4, resulting in reduced brain injury in a rodent stroke model.[47] Although Xu and colleagues found increased intracellular levels of miR-1906 in cultured astrocytes exposed to OGD, astrocyte-derived EVs revealed significantly reduced levels of miR-1906 after OGD induction. Nevertheless, the role of miR-1906 in MSC-derived EVs which were not directly exposed to hypoxia/ischemia, but which were preconditioned by lithium, has not yet been analyzed. We therefore first analyzed TLR4 protein expression patterns in astrocytes, neurons, and microglia cultured under standard cell culture conditions or exposed to OGD in the presence of PBS (control), EVs, or Li-EVs. Whereas TLR4 protein expression levels were low in all three cell types under standard cell culture conditions, induction of OGD yielded significantly increased protein levels in astrocytes, microglia, and neurons (Figure 5A-D). Treatment with EVs resulted in a nonsignificant trend toward a lower TLR4 expression in astrocytes, with virtually no trend in both neurons and microglia. Incubation of cells with Li-EVs, however, significantly reduced TLR4 protein expression in all three cell types, with an even more pronounced reduction of TLR4 in astrocytes (Figure 5A-D). Likewise, treatment of stroke mice with Li-EVs significantly decreased TLR4 expression patterns in the ischemic hemisphere, whereas native EVs had no impact on the protein expression (Figure 5E-F).
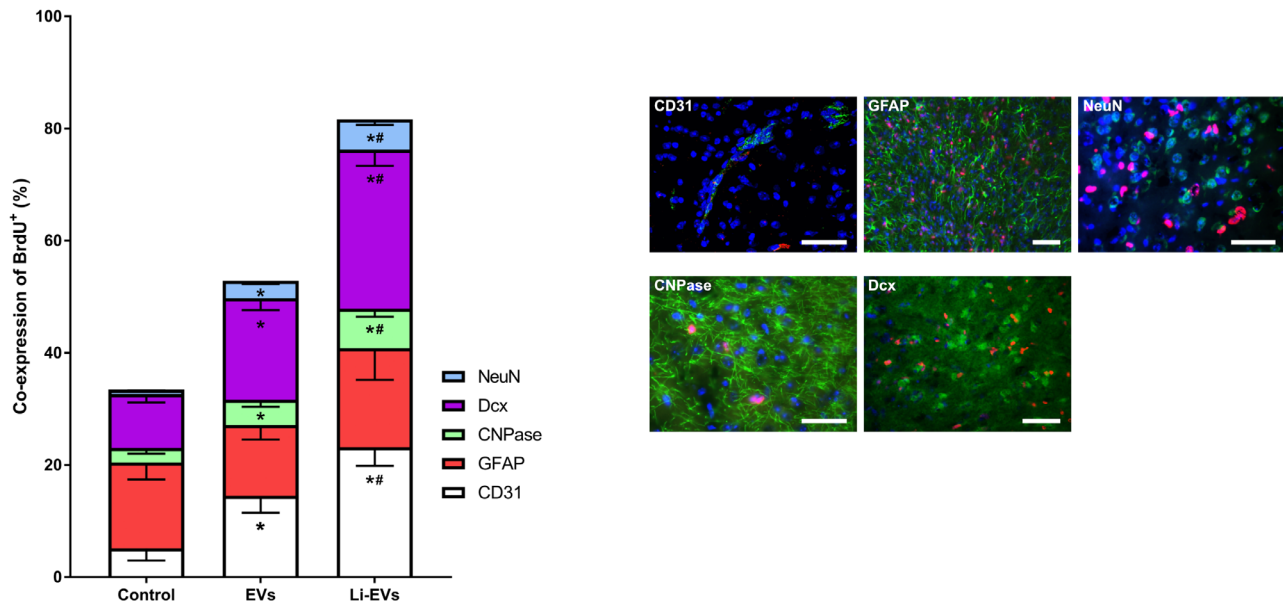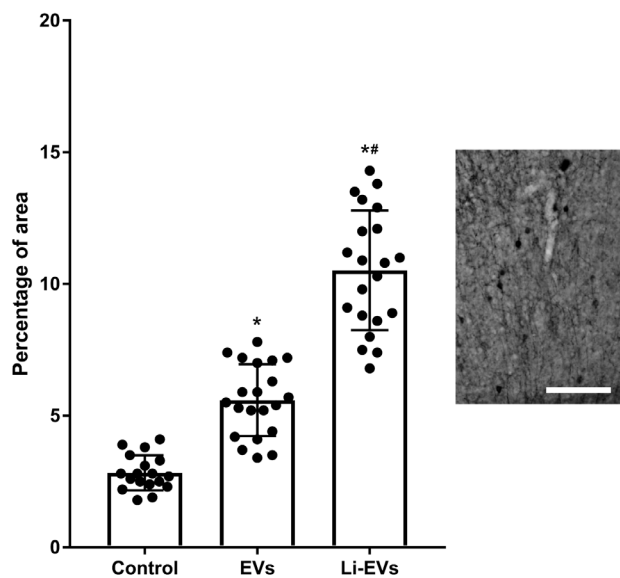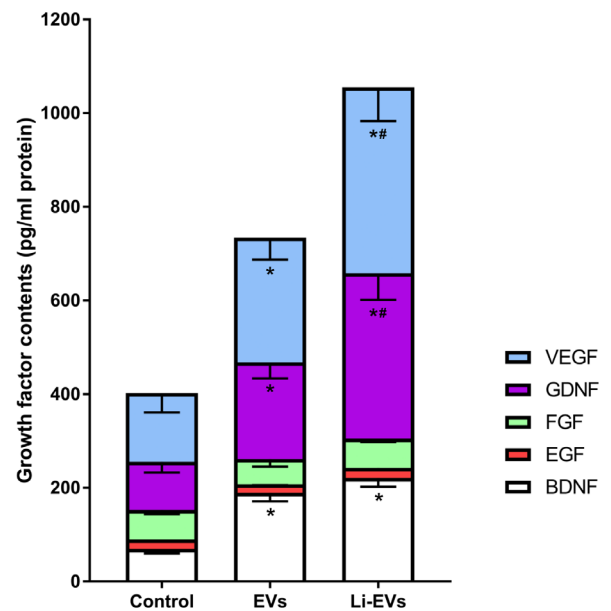
FIGURE 3 Treatment with Li-EVs enhances poststroke neuroregeneration and modifies poststroke extracellular milieu. Mice were exposed to middle cerebral artery occlusion followed by intravenous delivery of PBS (control), native EVs (EVs), or Li-EVs on days 1, 3, and 5. A, Differentiation patterns of BrdU+ cells were analyzed on day 84 within the ischemic hemisphere, using the neuronal markers Dcx and NeuN, the astroglial marker GFAP, the oligodendroglial marker CNPase, and the endothelial marker CD31. Representative photos taken from mice treated with Li-EVs depict the marker in question (green) plus BrdU+ cells (red) as well as the 4′,6-diamidino-2-phenylindole (DAPI) signal (blue). B, Poststroke axonal density was measured via stereotactic injection of the anterograde tract tracer BDA into the contralateral cortex 70 days after stroke. Axon labeling was performed within the ipsilateral hemisphere using DAB staining on day 84 poststroke. Axonal densities within the cortex of the ischemic hemisphere were measured from six fields per section out of eight sections of each mouse divided by total mean densities of all mice. A representative photo was taken from a mouse treated with Li-EVs. C, Concentrations of BDNF, EGF, FGF, GDNF, and VEGF were measured 3 months after the stroke within the ischemic hemisphere. Results are given as percentage of proportional areas. Scale bars for all photos are 50 μm. *Significantly different from controls ($P < .05$). #Significantly different from mice treated with native EVs ($P < 0.05$). n = 11-18 for controls, n = 8-21 for EVs, and n = 7-20 for Li-EVs. BDA, biotinylated dextran amine; BDNF, brain-derived neurotrophic factor; DAB, 3,3′-diaminobenzidine; Dcx, doublecortin; EGF, epidermal growth factor; EVs, extracellular vesicles; FGF fibroblast growth factor; GDNF, glial cell-derived neurotrophic factor; Li-EVs, lithium-treated EVs; PBS, phosphate-buffered saline; VEGF, vascular endothelial growth factor
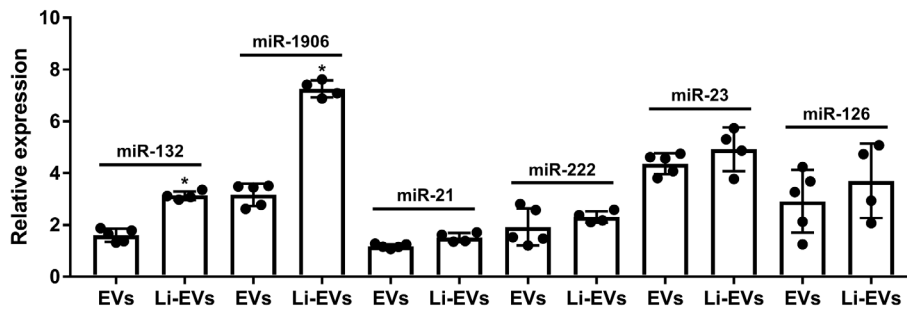
FIGURE 4 Measurement of selected miRNAs in MSC-derived EVs. Quantitative reverse transcription polymerase chain reaction (RT-qPCR) was used to measure miR-132, miR-1906, miR-21, miR-222, miR-23, and miR-126 levels in EV preparations derived from native MSCs (EVs) or lithium-preconditioned MSCs (Li-EVs) according to the manufacturer's protocols. Expression levels are normalized to MSCs = 1. *Significantly different from native MSC-derived EVs ($P < 0.05$). n = 5 for EVs and n = 4 for Li-EVs. EVs, extracellular vesicles; Li-EVs, lithium-treated EVs; MSC, mesenchymal stem cell

3.6 | Li-EVs reverse poststroke peripheral immunosuppression and reduce central inflammation

Previous work from our group has shown that delivery of native MSC-derived EVs induces sustained neurological recovery by reversal of peripheral poststroke immunosuppression at subacute stages of the disease, without inducing (sub)acute neuroprotection in these animals.[23] Likewise, similar effects are observed when stroke mice are treated with Li-EVs (Figure 6A,B). The latter reversed secondary immunosuppression on day 6, as indicated by flow cytometry from blood samples in these animals. However, no significant difference between treatment with native EVs and Li-EVs was observed. Analyzing poststroke immune responses within the ischemic brain, flow cytometry data revealed a decreased cerebral level of inflammation in animals treated with Li-EVs (Figure 6C,D), whereas native EVs had no impact on the ischemic cerebral immune response as previously described.[23]

3.7 | Li-EVs induce (sub)acute neuroprotection by interfering with the TLR4-dependent NF-κB signaling pathway

Since treatment with Li-EVs yielded a downregulation of the pro-inflammatory TLR4 under both in vitro and in vivo conditions (Figure 5), we next wondered whether or not changed TLR4 expression patterns result in activation of a plethora of different signaling pathways, among which is the NF-κB signaling pathway. However, we first analyzed whether or not the extent of poststroke brain injury is affected by treatment with Li-EVs. As shown in our previous work,[23] native EVs do not yield acute or subacute neuroprotection (Figure 7A-C), as observed by infarct volume analysis and TUNEL staining. In contrast to this, Li-EVs significantly reduced infarct volumes at both time points and reduced the number of TUNEL+ cells on day 6, further underlining the therapeutic impact of Li-EVs under experimental stroke conditions.

Li-EVs did not only reduce TLR4 expression patterns, but also modified the TLR4-dependent NF-κB pathway. As such, Li-EVs

inhibited the stroke-induced enhanced NF-κB signaling pathway, as indicated by decreased protein abundance of NF-kB p65 and increased protein abundance of IkB expression (Figure 7D,E). The application of native EVs had no impact in this context. Likewise, Li-EVs significantly reduced downstream proteasomal activity at 2 days poststroke, whereas no such effect was observed due to administration of native EVs (Figure 7F). Expression patterns of pro-inflammatory mediators such as iNOS and COX-2 were also significantly diminished by Li-EVs when compared with both controls and native EVs, resulting in reduced levels of TBARS in such animals (Figure 7G-I). Intracerebral concentrations of TNF-α were, however, not affected by the application of either Li-EVs or EVs (Figure 7J).

4 | DISCUSSION

The present study provides novel data on lithium-induced MSC preconditioning, changing the biological properties of such MSC-derived Li-EVs that results in increased intravesicular concentration of miR-1906. The latter modulates a recently established signaling pathway by reducing intracellular expression patterns of the pro-inflammatory TLR4 in cultured cells exposed to hypoxia and in the ischemic brain. TLR4 downregulation by Li-EVs, in turn, inhibits the NF-κB signaling pathway, decreases proteasomal activation and reduces both iNOS and COX-2 expression. Although native EVs do not affect poststroke cerebral inflammation directly but rather reverse peripheral immunosuppression, the increased therapeutic potential of Li-EVs over native EVs is a consequence of the combined impact on both peripheral and cerebral immune responses. A schematic summary of the suggested way of action is provided in Figure S2.

Lithium induces neuroprotection in preclinical stroke models. The majority of published work on such lithium-induced effects is hampered due to clinically irrelevant prestroke treatment, short-term observation periods, or insufficient insight into underlying mechanisms. As a matter of fact, studies using a prophylactic lithium delivery paradigm are restricted to rodent survival periods of 2 days only, thus focusing on a merely descriptive study design.[9,10] Although both Ren et al and Li et al chose a poststroke delivery protocol, lithium
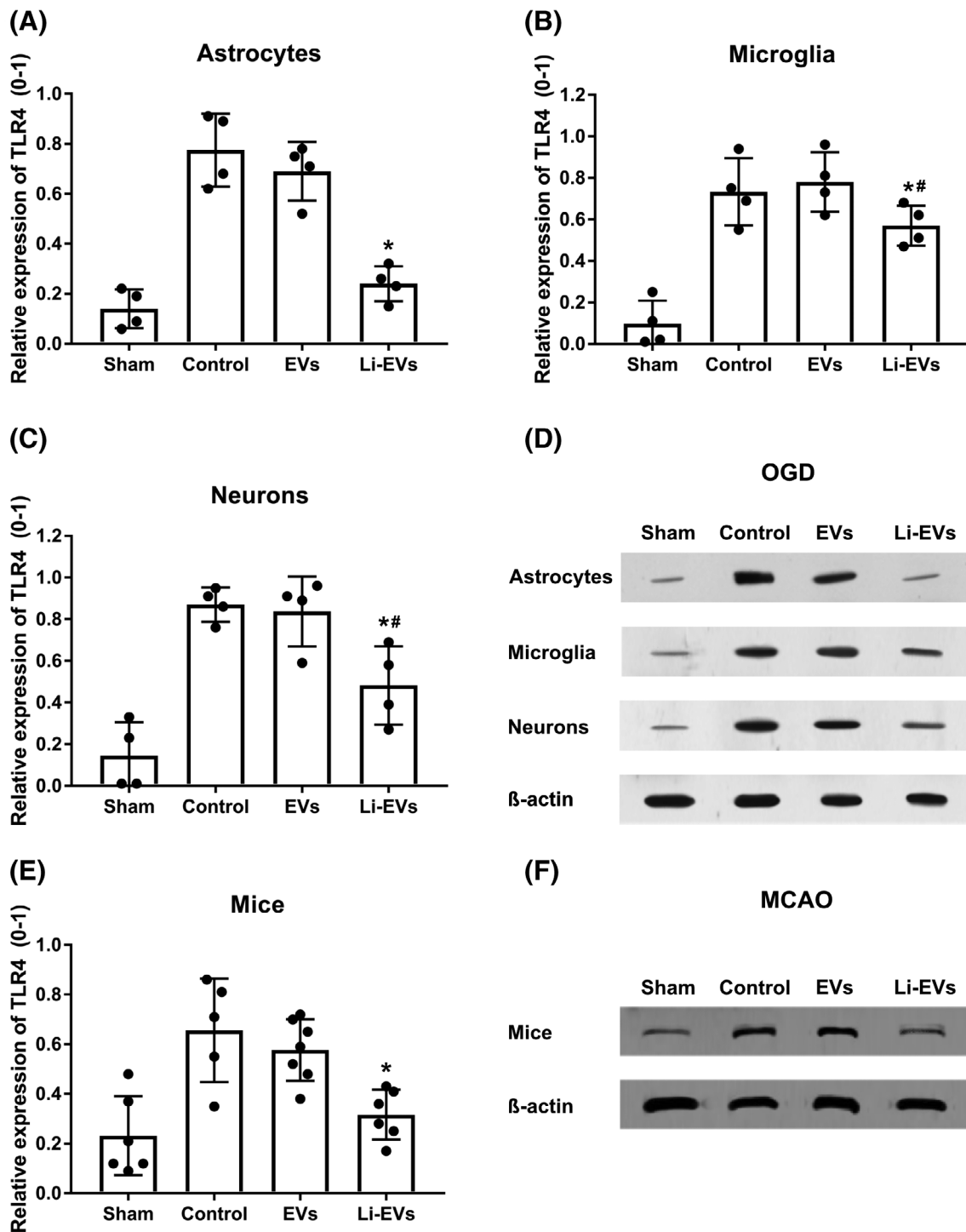
FIGURE 5 Li-EVs reduce expression of TLR4. Astrocytes, A, microglia, B, and neurons, C, were exposed to OGD injury followed by reoxygenation for 24 hours under standard cell culture conditions as described in materials and methods. Thereafter, the cells were lysed and used for Western blot analysis against TLR4 expression including densitometric analysis, D. Cells were treated with either PBS (control), native EVs (EVs), or Li-EVs at the beginning of the reoxygenation. Shams refer to cells kept under standard cell culture conditions without OGD and without any additional treatment. E,F TLR4 expression in left ischemic hemispheres 2 days after induction of cerebral ischemia in mice. The latter received single injections of PBS (control), EVs, or Li-EVs on day 1 after stroke. Sham mice underwent the same surgical procedure, but without inducing a stroke. Besides, sham mice did not receive any kind of additional treatment. *Significantly different from controls ($P < .05$). #Significantly different from shams ($P < .05$). n = 4 for each in vitro condition. n = 6 for sham mice, n = 5 for controls, n = 7 for EVs, and n = 6 for Li-EVs. EVs, extracellular vesicles; Li-EVs, lithium-treated EVs; OGD, oxygen-glucose-deprivation; PBS, phosphate-buffered saline; TLR4, toll-like-receptor-4
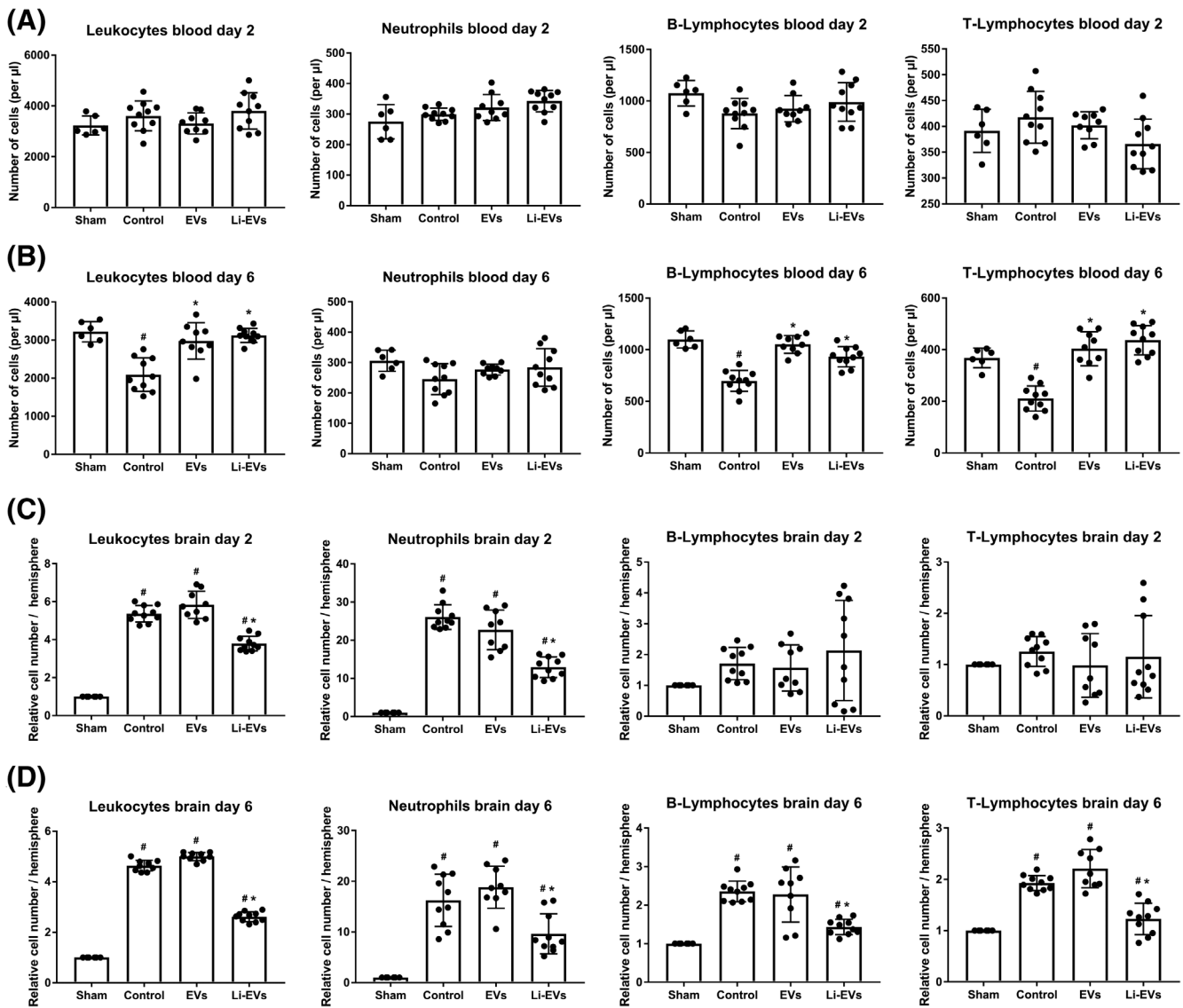
FIGURE 6 Application of Li-EVs reverses poststroke immunosuppression and reduces cerebral immune responses. Flow cytometry analysis was performed from both blood samples, A,B, and from left ischemic brain hemispheres, C,D, on day 2, A,C, and on day 6, B,D, after induction of stroke. Sham animals underwent surgical procedure for transient focal cerebral ischemia without inserting the filament into the left middle cerebral artery and without any treatment. On the contrary, control animals received one intravenous injection of PBS for the 2-day survival period, A,C, or three injections on days 1, 3, and 5, B,D, for the 6-day survival period. Likewise, both EVs or Li-EVs were given intravenously only once for the 2-day survival period, A,C, or three times for the 6-day survival period, B,D. Quantitative analyses were performed for the detection of total numbers of leukocytes, neutrophils, B-lymphocytes, and T-lymphocytes. For flow cytometry analysis in blood samples, absolute amounts of cells in question are given, whereas cell numbers from left ischemic hemispheres refer to left hemispheres from sham animals set as 1. *Significantly different from controls ($P < .05$). #Significantly different from sham mice or from mice treated with native EVs ($P < .05$). n = 6 for sham mice, n = 10 for controls, n = 9 for EVs, and n = 10 for Li-EVs. EVs, extracellular vesicles; Li-EVs, lithium-treated EVs

administration was still limited in terms of time frame with lithium being given no later than 3 hours poststroke.[11,12] It was not until recently when the aforementioned therapeutic time window was significantly extended toward 6 hours, albeit such a time window is still inferior to neuroregenerative approaches when compared with MSC transplantation.[13]

The transplantation of MSCs yields increased neurological recovery in preclinical stroke models with therapeutic time windows ranging to days or even longer.[26,57-59] Although clinical trials have recently

been performed, the benefit for stroke patients due to MSC transplantation still needs further evaluation.[60-63] As a matter of fact, cell transplantation suffers from the same setbacks as is the case for endogenous stem cells. Furthermore, transplantation of ectopic stem cells may include additional hazards such as neoplastic transformation, immunological reactions, or thromboembolic events during cell infusion.[64,65] Previous work therefore focused on enhancing MSC resistance against the postischemic pro-inflammatory milieu. In this context, preconditioning of MSCs with the mood stabilizers lithium or
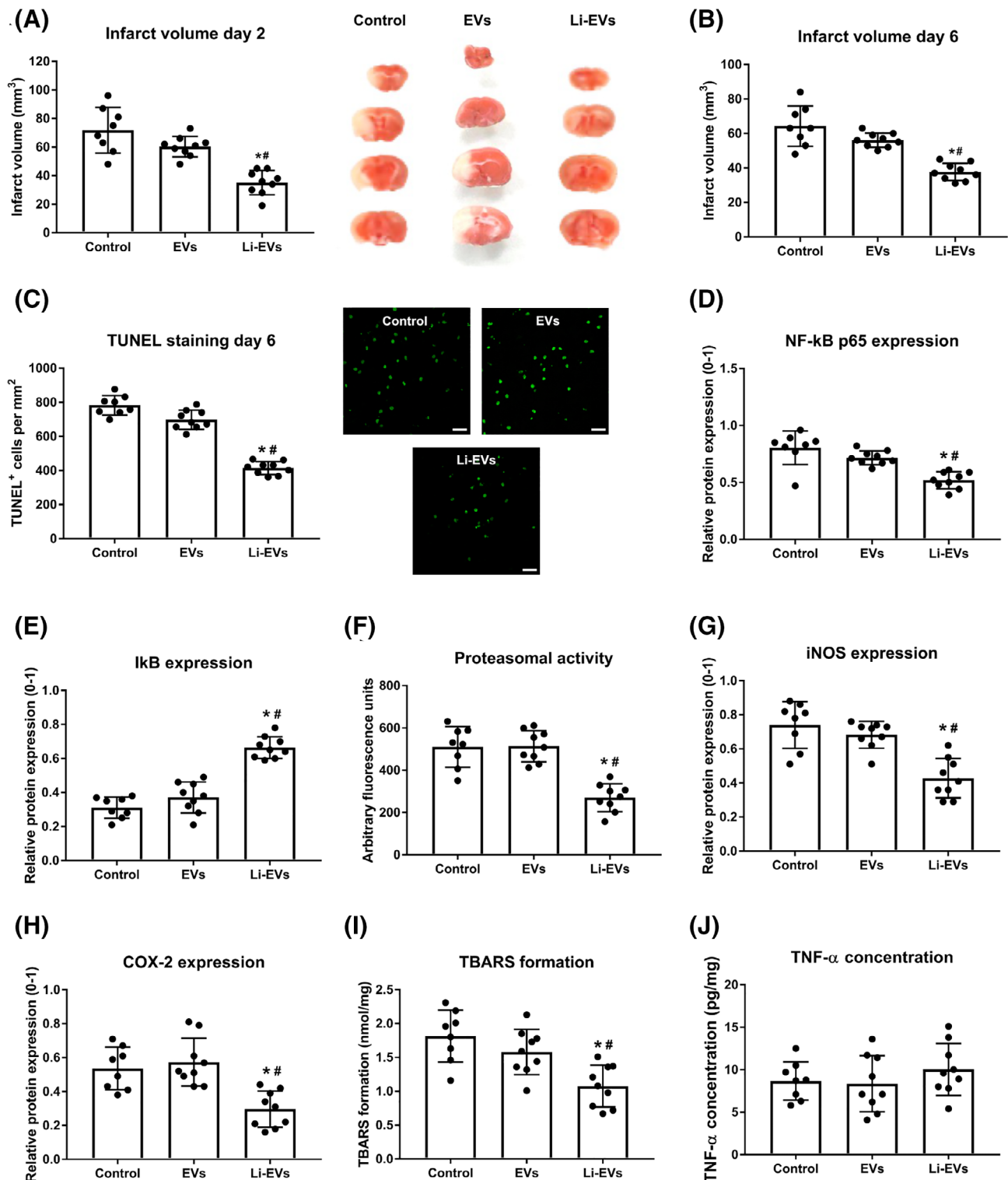
FIGURE 7 Application of Li-EVs results in modification of distinct signaling pathways upon stroke induction. Mice were exposed to stroke followed by intravenous delivery of either PBS (control), native EVs (EVs), or Li-EVs. Except for infarct volume analysis and TUNEL staining on day 6, B,C, where mice received intravenous injections on days 1, 3, and 5, animals received one single treatment on day 1 only, followed by sacrifice of these animals 2 days after stroke induction. As such, infarct volumes were determined on day 2, A, and on day 6, B, whereas TUNEL staining was performed on day 6 only, C. NF-κB p65, D, and IκB-α, E, expression, proteasome activity, F, inducible NO synthase, G, and COX-2, H, expression, TBARS formation, I, and tumor necrosis factor-α, J, were analyzed on day 2 after stroke induction. Scale bars: 50 μm. *Significantly different from controls ($P < .05$). #Significantly different from mice treated with native EVs ($P < .05$). n = 8 for controls, n = 9 for EVs, and n = 9 for Li-EVs. COX-2, cyclooxygenase-2; EVs, extracellular vesicles; Li-EVs, lithium-treated EVs; iNOS, inducible NO synthase; PBS, phosphate-buffered saline; TBARS, thiobarbituric acid reactive substances; TNF-α, tumor necrosis factor-α

valproic acid (VPA) has been shown to enhance the therapeutic potential of such preconditioned MSCs in preclinical models of Huntington's disease and stroke.[21,22,31] Tsai and colleagues observed increased migratory properties when MSCs were preconditioned with either VPA or lithium, and the combination of the two enhanced the migratory characteristics of such preconditioned MSCs even further.[22] Increased homing after poststroke transplantation of preconditioned MSCs yielded better neurological recovery, reduced brain injury, and stimulated endogenous angiogenesis, all of which being a consequence of affecting the chemokine receptor 4 and matrix metalloprotease 9 activity, as discussed by the authors.[22] Nevertheless, MSCs are known to act in an indirect way, using paracrine mechanisms like the secretion of EVs in order to exert their neuroprotective or neuroregenerative effects. Hence, enhanced MSC homing properties due to preconditioning with lithium or VPA are of minor relevance when EVs instead of MSCs can be used, thus circumventing any potential side effects of stem cell transplantation itself.

EVs from various cell sources have been successfully applied in preclinical stroke models.[23,28-30,66-68] Although the precise mechanisms by which EVs induce neuroprotection or neuroregeneration along with better neurological recovery remain elusive, evidence suggests that EVs might predominantly interfere with secondary immune responses rather than induce enhanced neuronal cell survival directly.[69-72] In this context, previous work from our own group has shown that native MSC-derived EVs improve neurological recovery and neuroregeneration by reversing peripheral poststroke immunosuppression, without reducing (sub)acute brain injury or cerebral inflammation.[23] The lack of acute neuroprotection in vivo along with increased neurological recovery, stimulated neuroregeneration, and the reversal of peripheral poststroke immunosuppression by native EVs as observed in the present work is therefore in line with our previous observation. Preconditioning with lithium yields similar results with regard to these aspects, but the impact of Li-EVs appears to be superior to the delivery of native EVs. On the contrary, the application of Li-EVs is associated with both acute neuroprotection and reduced levels of cerebral inflammation in stroke mice. The reduction of poststroke cerebral inflammation as observed in mice treated with Li-EVs thus likely contributes to acute neuroprotection, which in turn results in overall better neurological recovery together with the reversal of peripheral immunosuppression. Noteworthy, not only Li-EVs but also native EVs protect cultured neurons from hypoxic injury. The latter appears to be surprising, since native EVs are supposed to not affect acute cell survival but only act via peripheral immune reactions, which are of course not present in a cell culture model. However, recent data indicate that native EVs might also induce acute neuroprotection to some extent via antiapoptotic actions and via modulation of related signaling cascades.[68,73,74] Elucidating such additional apoptotic pathways, however, was beyond the scope of the present work.

Preconditioning of cultured MSCs with lithium enhances the therapeutic potential of such enriched EVs under both in vitro and in vivo conditions, as has been observed for other preconditioning paradigms such as hypoxic MSC conditioning.[75] Since miRNAs are one key mediator of EV-induced biological effects, we hypothesized that lithium preconditioning might affect EV secretion profiles with regard to miRNA contents. Indeed, both miR-132 and miR-1906 were significantly increased in Li-EVs. Although the former has been described to stimulate tissue regeneration in a model of myocardial infarction,[44] previous unpublished observation of our own yielded no such impact in the stroke model. On the contrary, miR-1906 has just recently been realized to be a critical mediator of neuroprotection in a mouse model of cerebral ischemia.[47] Xu and colleagues described stroke-enriched intracellular levels of miR-1906 in both neurons and even more so in glial cells. Intravesicular concentrations of miR-1906 from glial cell-derived EVs, however, were significantly decreased, suggesting an insufficient concentration of miR-1906 in order to yield enhanced resistance of neurons against ischemic stress. As such, ectopic delivery of miR-1906 resulted in significant neuroprotection by a hitherto unknown mechanism of miR-1906, inhibiting the pro-inflammatory TLR4 signaling pathway.[47] In line with this, our work found increased levels of intravesicular miR-1906 after lithium preconditioning inhibiting the aforementioned TLR4 pathway as well.

The importance of the TLR4 for generating ischemic injury under experimental conditions has already been established for more than 10 years.[76] Nevertheless, the modulation of that pathway due to lithium in MSC-derived EVs by miR-1906 has not been shown, yet. Following the inhibition of TLR4 by Li-EVs after both hypoxia and cerebral ischemia, such reduced TLR4 levels yield an inhibition of the NF-κB signaling pathway which give rise to reduced poststroke proteasomal activities. The latter has been found to be critically involved in ischemic injury of the brain and other organs as well.[77-80] Along with this, Li-EVs significantly reduce levels of both iNOS and COX-2 expression, all of which contributing to reduction of cerebral inflammation as well as neuronal injury, which has been described afore.[76]

In conclusion, preconditioning of MSCs with lithium yields biologically highly active Li-EVs, providing profound neuroprotection and neurological recovery in a mouse model of cerebral ischemia. Hence, these beneficial effects of Li-EVs are a consequence of a plethora of mechanisms, among which the reversal of peripheral immunosuppression and the inhibition of TLR4-dependent signaling pathways are prominent. Additional experimental studies are in order to further validate these underlying mechanisms by which Li-EVs grant neurological recovery upon induction of cerebral ischemia.

CONFLICT OF INTEREST

B.B. declared employment/leadership position with Mediclin Klinik Reichshof, NNFR&W. The other authors declared no potential conflicts of interest.

AUTHOR CONTRIBUTIONS

M.H., X.Z.: collection and assembly of data, data analysis and interpretation, manuscript writing, final approval of manuscript; Y.K., S.L.: collection and assembly of data, data analysis and interpretation, final

ORCID

Matteo Haupt https://orcid.org/0000-0002-6067-4563
Thorsten R. Doeppner https://orcid.org/0000-0002-1222-9211

REFERENCES

1. Manji HK, Lenox RH. Lithium: a molecular transducer of mood-stabilization in the treatment of bipolar disorder. *Neuropsychopharmacology*. 1998;19(3):161-166.
2. Yu F, Wang Z, Tchantchou F, Chiu CT, Zhang Y, Chuang DM. Lithium ameliorates neurodegeneration, suppresses neuroinflammation, and improves behavioral performance in a mouse model of traumatic brain injury. *J Neurotrauma*. 2012;29(2):362-374.
3. Kang K, Kim YJ, Kim YH, et al. Lithium pretreatment reduces brain injury after intracerebral hemorrhage in rats. *Neurol Res*. 2012;34(5):447-454.
4. Wang ZF, Fessler EB, Chuang DM. Beneficial effects of mood stabilizers lithium, valproate and lamotrigine in experimental stroke models. *Acta Pharmacol Sin*. 2011;32(12):1433-1445.
5. Yu F, Wang Z, Tanaka M, et al. Posttrauma cotreatment with lithium and valproate: reduction of lesion volume, attenuation of blood-brain barrier disruption, and improvement in motor coordination in mice with traumatic brain injury. *J Neurosurg*. 2013;119(3):766-773.
6. Chiu CT, Chuang DM. Molecular actions and therapeutic potential of lithium in preclinical and clinical studies of CNS disorders. *Pharmacol Ther*. 2010;128(2):281-304.
7. Aggarwal SP, Zinman L, Simpson E, et al. Safety and efficacy of lithium in combination with riluzole for treatment of amyotrophic lateral sclerosis: a randomised, double-blind, placebo-controlled trial. *Lancet Neurol*. 2010;9(5):481-488.
8. Mohammadianinejad SE, Majdinasab N, Sajedi SA, Abdollahi F, Moqaddam MM, Sadr F. The effect of lithium in post-stroke motor recovery: a double-blind, placebo-controlled, randomized clinical trial. *Clin Neuropharmacol*. 2014;37(3):73-78.
9. Nonaka S, Chuang DM. Neuroprotective effects of chronic lithium on focal cerebral ischemia in rats. *Neuroreport*. 1998;9(9):2081-2084.
10. Xu J, Culman J, Blume A, Brecht S, Gohlke P. Chronic treatment with a low dose of lithium protects the brain against ischemic injury by reducing apoptotic death. *Stroke*. 2003;34(5):1287-1292.
11. Li H, Li Q, Du X, et al. Lithium-mediated long-term neuroprotection in neonatal rat hypoxia-ischemia is associated with antiinflammatory effects and enhanced proliferation and survival of neural stem/progenitor cells. *J Cereb Blood Flow Metab*. 2011;31(10):2106-2115.
12. Ren M, Senatorov VV, Chen RW, Chuang DM. Postinsult treatment with lithium reduces brain damage and facilitates neurological recovery in a rat ischemia/reperfusion model. *Proc Natl Acad Sci*. 2003;100 (10):6210-6215.
13. Doeppner TR, Kaltwasser B, Sanchez-Mendoza EH, Caglayan AB, Bähr M, Hermann DM. Lithium-induced neuroprotection in stroke involves increased miR-124 expression, reduced RE1-silencing transcription factor abundance and decreased protein deubiquitination by GSK3beta inhibition-independent pathways. *J Cereb Blood Flow Metab*. 2017;37(3):914-926.
14. Doeppner TR, Ewert TAS, Tönges L, et al. Transduction of neural precursor cells with TAT-heat shock protein 70 chaperone: therapeutic potential against ischemic stroke after intrastriatal and systemic transplantation. *Stem Cells*. 2012;30(6):1297-1310.
15. Doeppner TR, Hermann DM. Mesenchymal stem cells in the treatment of ischemic stroke: progress and possibilities. *Stem Cells Cloning Adv Appl*. 2010;3:157-163.
16. Doeppner TR, Kaltwasser B, Teli MK, Bretschneider E, Bähr M, Hermann DM. Effects of acute versus post-acute systemic delivery of neural progenitor cells on neurological recovery and brain remodeling after focal cerebral ischemia in mice. *Cell Death Dis*. 2014;5(8):e1386.
17. Chen J, Li Y, Katakowski M, et al. Intravenous bone marrow stromal cell therapy reduces apoptosis and promotes endogenous cell proliferation after stroke in female rat. *J Neurosci Res*. 2003;73(6):778-786.
18. Li Y, Chen J, Wang L, Lu M, Chopp M. Treatment of stroke in rat with intracarotid administration of marrow stromal cells. *Neurology*. 2001;56(12):1666-1672.
19. Hermann DM, Peruzzotti-Jametti L, Schlechter J, et al. Neural precursor cells in the ischemic brain - integration, cellular crosstalk, and consequences for stroke recovery. *Front Cell Neurosci*. 2014;8:291.
20. Hermann DM, Chopp M. Promoting brain remodelling and plasticity for stroke recovery: therapeutic promise and potential pitfalls of clinical translation. *Lancet Neurol*. 2012;11(4):369-380.
21. Linares GR, Chiu CT, Scheuing L, et al. Preconditioning mesenchymal stem cells with the mood stabilizers lithium and valproic acid enhances therapeutic efficacy in a mouse model of Huntington's disease. *Exp Neurol*. 2016;281:81-92.
22. Tsai LK, Wang Z, Munasinghe J, Leng Y, Leeds P, Chuang DM. Mesenchymal stem cells primed with valproate and lithium robustly migrate to infarcted regions and facilitate recovery in a stroke model. *Stroke*. 2011;42(10):2932-2939.
23. Doeppner TR, Herz J, Gorgens A, et al. Extracellular vesicles improve post-stroke neuroregeneration and prevent postischemic immunosuppression. *Stem Cells Transl Med*. 2015;4(10):1131-1143.
24. Arslan F, Lai RC, Smeets MB, et al. Mesenchymal stem cell-derived exosomes increase ATP levels, decrease oxidative stress and activate PI3K/Akt pathway to enhance myocardial viability and prevent adverse remodeling after myocardial ischemia/reperfusion injury. *Stem Cell Res*. 2013;10(3):301-312.
25. Bian S, Zhang L, Duan L, Wang X, Min Y, Yu H. Extracellular vesicles derived from human bone marrow mesenchymal stem cells promote angiogenesis in a rat myocardial infarction model. *J Mol Med*. 2014;92 (4):387-397.
26. Chen KH, Chen CH, Wallace CG, et al. Intravenous administration of xenogenic adipose-derived mesenchymal stem cells (ADMSC) and ADMSC-derived exosomes markedly reduced brain infarct volume and preserved neurological function in rat after acute ischemic stroke. *Oncotarget*. 2016;7(46):74537-74556.
27. Thery C, Witwer KW, Aikawa E, et al. Minimal information for studies of extracellular vesicles 2018 (MISEV2018): a position statement of the International Society for Extracellular Vesicles and update of the MISEV2014 guidelines. *J Extracell Vesicles*. 2018;7(1):1535750.
28. Xin H, Li Y, Cui Y, Yang JJ, Zhang ZG, Chopp M. Systemic administration of exosomes released from mesenchymal stromal cells promote functional recovery and neurovascular plasticity after stroke in rats. *J Cereb Blood Flow Metab*. 2013;33(11):1711-1715.
29. Deng M, Xiao H, Zhang H, et al. Mesenchymal stem cell-derived extracellular vesicles ameliorates hippocampal synaptic impairment after transient global ischemia. *Front Cell Neurosci*. 2017;11:205.
30. Otero-Ortega L, Laso-Garcia F, Gomez-de Frutos MD, et al. White matter repair after extracellular vesicles administration in an experimental animal model of subcortical stroke. *Sci Rep*. 2017;7:44433.

31. Tsai LK, Leng Y, Wang Z, Leeds P, Chuang DM. The mood stabilizers valproic acid and lithium enhance mesenchymal stem cell migration via distinct mechanisms. *Neuropsychopharmacology*. 2010;35(11): 2225-2237.

32. Ludwig AK, De Miroschedji K, Doeppner TR, et al. Precipitation with polyethylene glycol followed by washing and pelleting by ultracentrifugation enriches extracellular vesicles from tissue culture supernatants in small and large scales. *J Extracell Vesicles*. 2018;7(1):1528109.

33. Sokolova V, Ludwig AK, Hornung S, et al. Characterisation of exosomes derived from human cells by nanoparticle tracking analysis and scanning electron microscopy. *Colloids Surf B Biointerfaces*. 2011; 87(1):146-150.

34. Doeppner TR, Doehring M, Kaltwasser B, et al. Ischemic post-conditioning induces post-stroke neuroprotection via Hsp70-mediated proteasome inhibition and facilitates neural progenitor cell transplantation. *Mol Neurobiol*. 2017;54(8):6061-6073.

35. Wang YC, Dzyubenko E, Sanchez-Mendoza EH, et al. Postacute delivery of GABAA α5 antagonist promotes postischemic neurological recovery and peri-infarct brain remodeling. *Stroke*. 2018;49(10):2495-2503.

36. Doeppner TR, Kaltwasser B, Bähr M, et al. Effects of neural progenitor cells on post-stroke neurological impairment—a detailed and comprehensive analysis of behavioral tests. *Front Cell Neurosci*. 2014; 8:338.

37. Balkaya MG, Trueman RC, Boltze J, Corbett D, Jolkkonen J. Behavioral outcome measures to improve experimental stroke research. *Behav Brain Res*. 2018;352:161-171.

38. Doeppner TR, Mlynarczuk-Bialy I, Kuckelkorn U, et al. The novel proteasome inhibitor BSc2118 protects against cerebral ischaemia through HIF1A accumulation and enhanced angioneurogenesis. *Brain*. 2012;135(Pt 11):3282-3297.

39. Chu HX, Kim HA, Lee S, et al. Immune cell infiltration in malignant middle cerebral artery infarction: comparison with transient cerebral ischemia. *J Cereb Blood Flow Metab*. 2014;34(3):450-459.

40. Doeppner TR, Kaltwasser B, Fengyan J, Hermann DM, Bähr M. TAT-Hsp70 induces neuroprotection against stroke via anti-inflammatory actions providing appropriate cellular microenvironment for transplantation of neural precursor cells. *J Cereb Blood Flow Metab*. 2013; 33(11):1778-1788.

41. Safwat A, Sabry D, Ragiae A, et al. Adipose mesenchymal stem cells-derived exosomes attenuate retina degeneration of streptozotocin-induced diabetes in rabbits. *J Circ Biomark*. 2018;7: 1849454418807827.

42. Ching RC, Wiberg M, Kingham PJ. Schwann cell-like differentiated adipose stem cells promote neurite outgrowth via secreted exosomes and RNA transfer. *Stem Cell Res Ther*. 2018;9(1):266.

43. Qiu G, Zheng G, Ge M, et al. Mesenchymal stem cell-derived extracellular vesicles affect disease outcomes via transfer of microRNAs. *Stem Cell Res Ther*. 2018;9(1):320.

44. Ma T, Chen Y, Chen Y, et al. MicroRNA-132, delivered by mesenchymal stem cell-derived exosomes, promote angiogenesis in myocardial infarction. *Stem Cells Int*. 2018;2018:3290372.

45. Hwang JY, Kaneko N, Noh KM, Pontarelli F, Zukin RS. The gene silencing transcription factor REST represses miR-132 expression in hippocampal neurons destined to die. *J Mol Biol*. 2014;426(20):3454-3466.

46. Zhang Y, Han B, He Y, et al. MicroRNA-132 attenuates neurobehavioral and neuropathological changes associated with intracerebral hemorrhage in mice. *Neurochem Int*. 2017;107:182-190.

47. Xu X, Wen Z, Zhao N, et al. MicroRNA-1906, a novel regulator of Toll-like receptor 4, ameliorates ischemic injury after experimental stroke in mice. *J Neurosci*. 2017;37(43):10498-10515.

48. Pan Q, Zheng J, Du D, et al. MicroRNA-126 priming enhances functions of endothelial progenitor cells under physiological and hypoxic conditions and their therapeutic efficacy in cerebral ischemic damage. *Stem Cells Int*. 2018;2018:1-13.

49. Shan C, Ma Y. MicroRNA-126/stromal cell-derived factor 1/C-X-C chemokine receptor type 7 signaling pathway promotes post-stroke angiogenesis of endothelial progenitor cell transplantation. *Mol Med Rep*. 2018;17(4):5300-5305.

50. Chen J, Cui C, Yang X, et al. MiR-126 affects brain-heart interaction after cerebral ischemic stroke. *Transl Stroke Res*. 2017;8(4):374-385.

51. Bazan HA, Hatfield SA, O'Malley CB, Brooks AJ, Lightell D Jr, Woods TC. Acute loss of miR-221 and miR-222 in the atherosclerotic plaque shoulder accompanies plaque rupture. *Stroke*. 2015;46(11): 3285-3287.

52. Yao X, Wang Y, Zhang D. microRNA-21 confers neuroprotection against cerebral ischemia-reperfusion injury and alleviates blood-brain barrier disruption in rats via the MAPK signaling pathway. *J Mol Neurosci*. 2018;65(1):43-53.

53. Wang W, Li DB, Li RY, et al. Diagnosis of hyperacute and acute ischaemic stroke: the potential utility of exosomal microRNA-21-5p and microRNA-30a-5p. *Cerebrovasc Dis*. 2018;45(5–6):204-212.

54. Li JS, Yao ZX. MicroRNAs: novel regulators of oligodendrocyte differentiation and potential therapeutic targets in demyelination-related diseases. *Mol Neurobiol*. 2012;45(1):200-212.

55. Mateescu B, Kowal EJ, van Balkom BW, et al. Obstacles and opportunities in the functional analysis of extracellular vesicle RNA—an ISEV position paper. *J Extracell Vesicles*. 2017;6(1):1286095.

56. Doeppner TR, Doehring M, Bretschneider E, et al. MicroRNA-124 protects against focal cerebral ischemia via mechanisms involving Usp14-dependent REST degradation. *Acta Neuropathol*. 2013;126(2): 251-265.

57. Ullah I, Subbarao RB, Rho GJ. Human mesenchymal stem cells—current trends and future prospective. *Biosci Rep*. 2015;35(2):e00191.

58. Wei ZZ, Gu X, Ferdinand A, et al. Intranasal delivery of bone marrow mesenchymal stem cells improved neurovascular regeneration and rescued neuropsychiatric deficits after neonatal stroke in rats. *Cell Transplant*. 2015;24(3):391-402.

59. Komatsu K, Honmou O, Suzuki J, Houkin K, Hamada H, Kocsis JD. Therapeutic time window of mesenchymal stem cells derived from bone marrow after cerebral ischemia. *Brain Res*. 2010;1334:84-92.

60. Bhasin A, Srivastava MV, Kumaran SS, et al. Autologous mesenchymal stem cells in chronic stroke. *Cerebrovasc Dis Extra*. 2011;1(1):93-104.

61. Honmou O, Houkin K, Matsunaga T, et al. Intravenous administration of auto serum-expanded autologous mesenchymal stem cells in stroke. *Brain*. 2011;134(Pt 6):1790-1807.

62. Lee JS, Hong JM, Moon GJ, et al. A long-term follow-up study of intravenous autologous mesenchymal stem cell transplantation in patients with ischemic stroke. *STEM CELLS*. 2010;28(6):1099-1106.

63. Hess DC, Wechsler LR, Clark WM, et al. Safety and efficacy of multipotent adult progenitor cells in acute ischaemic stroke (MASTERS): a randomised, double-blind, placebo-controlled, phase 2 trial. *Lancet Neurol*. 2017;16(5):360-368.

64. Boltze J, Arnold A, Walczak P, et al. The dark side of the force—constraints and complications of cell therapies for stroke. *Front Neurol*. 2015;6:155.

65. Cui LL, Kerkela E, Bakreen A, et al. The cerebral embolism evoked by intra-arterial delivery of allogeneic bone marrow mesenchymal stem cells in rats is related to cell dose and infusion velocity. *Stem Cell Res Ther*. 2015;6(1):11.

66. Xin H, Katakowski M, Wang F, et al. MicroRNA cluster miR-17-92 cluster in exosomes enhance neuroplasticity and functional recovery after stroke in rats. *Stroke*. 2017;48(3):747-753.

67. Xin H, Li Y, Chopp M. Exosomes/miRNAs as mediating cell-based therapy of stroke. *Front Cell Neurosci*. 2014;8:377.

68. Deng M, Xiao H, Peng H, et al. Preservation of neuronal functions by exosomes derived from different human neural cell types under ischemic conditions. *Eur J Neurosci*. 2018;47(2):150-157.

69. Dabrowska S, Andrzejewska A, Strzemecki D, Muraca M, Janowski M, Lukomska B. Human bone marrow mesenchymal stem cell-derived

extracellular vesicles attenuate neuroinflammation evoked by focal brain injury in rats. *J Neuroinflammation*. 2019;16(1):216.

70. Dabrowska S, Andrzejewska A, Lukomska B, Janowski M. Neuroinflammation as a target for treatment of stroke using mesenchymal stem cells and extracellular vesicles. *J Neuroinflammation*. 2019;16 (1):178.

71. Doeppner TR, Bähr M, Giebel B, et al. Immunological and non-immunological effects of stem cell-derived extracellular vesicles on the ischaemic brain. *Ther Adv Neurol Disorder*. 2018;11: 1756286418789326.

72. Venkat P, Chen J, Chopp M. Exosome-mediated amplification of endogenous brain repair mechanisms and brain and systemic organ interaction in modulating neurological outcome after stroke. *J Cereb Blood Flow Metab*. 2018;38(12):2165-2178.

73. Joerger-Messerli MS, Oppliger B, Spinelli M, et al. Extracellular vesicles derived from Wharton's jelly mesenchymal stem cells prevent and resolve programmed cell death mediated by perinatal hypoxia-ischemia in neuronal cells. *Cell Transplant*. 2018;27(1):168-180.

74. Ophelders DR, Wolfs TG, Jellema RK, et al. Mesenchymal stromal cell-derived extracellular vesicles protect the fetal brain after hypoxia-ischemia. *Stem Cells Transl Med*. 2016;5(6):754-763.

75. Jiang RH, Wu CJ, Xu XQ, et al. Hypoxic conditioned medium derived from bone marrow mesenchymal stromal cells protects against ischemic stroke in rats. *J Cell Physiol*. 2018;234(2):1354-1368.

76. Caso JR, Pradillo JM, Hurtado O, et al. Toll-like receptor 4 is involved in brain damage and inflammation after experimental stroke. *Circulation*. 2007;115(12):1599-1608.

77. Doeppner TR, Kaltwasser B, Kuckelkorn U, et al. Systemic proteasome inhibition induces sustained post-stroke neurological recovery and neuroprotection via mechanisms involving reversal of peripheral immunosuppression and preservation of blood-brain-barrier integrity. *Mol Neurobiol*. 2016;53(9):6332-6341.

78. Zhang L, Zhang ZG, Liu X, et al. Treatment of embolic stroke in rats with bortezomib and recombinant human tissue plasminogen activator. *Thromb Haemost*. 2006;95(1):166-173.

79. Zhang Y, Xiong M, Yan RQ, Sun FY. Mutant ubiquitin-mediated beta-secretase stability via activation of caspase-3 is related to beta-amyloid accumulation in ischemic striatum in rats. *J Cereb Blood Flow Metab*. 2010;30(3):566-575.

80. Phillips JB, Williams AJ, Adams J, et al. Proteasome inhibitor PS519 reduces infarction and attenuates leukocyte infiltration in a rat model of focal cerebral ischemia. *Stroke*. 2000;31(7):1686-1693.

SUPPORTING INFORMATION

Additional supporting information may be found online in the Supporting Information section at the end of this article.